The effects of elastic cycling in nanoindentation of a metallic glass

C. M. Meylan & A. L. Greer

Published online: 15 Sep 2020.

Submit your article to this journal ⬀

Article views: 168

View related articles ⬀

View Crossmark data ⬀

The effects of elastic cycling in nanoindentation of a metallic glass

C. M. Meylan [ORCID] and A. L. Greer [ORCID]

Department of Materials Science & Metallurgy, University of Cambridge, Cambridge, UK

ABSTRACT

We use nanoindentation to perform elastic cycling on, and to characterise, the bulk metallic glass $Cu_{46}Zr_{46}Al_7Gd_1$. From multiple loading curves, cumulative distributions are determined for several properties, including the initial yield load, the hardness and the indentation modulus. The distributions are characterised by the median property value and by their width. The effects of elastic cycling under the indenter tip are compared with those of annealing and of cryogenic thermal cycling applied to the bulk glass. We confirm that elastic cycling significantly increases the initial yield load, and find evidence for localised strengthening. In the first reports of this apparent strengthening, it was attributed to stimulation of relaxation of the glass to a more ordered structure, an effect that would be similar to that of annealing. In contrast, we conclude that the increased yield load is not due to structural ordering in the glass, but to compressive residual stress resulting from anelastic strains. While there may be effects of elastic cycling on the structure of metallic glasses, these are not revealed by loading in nanoindentation.

1. Introduction

The elastic behaviour of metallic glasses (MGs) is complex, because each atom in a glass has a unique surrounding. The shear modulus of MGs is significantly less than that of their crystalline counterparts. Weaire et al. showed that this could be explained by internal atomic rearrangements contributing to the shear strain [1]. X-ray diffraction studies of MGs under elastic loading show that the pair distribution functions do not remain self-similar [2–4]; the atomic displacements must have a significant non-affine component. Molecular-dynamics simulations show that the inhomogeneity of the elastic response can be correlated with the local short-range order [5].

In the elastic regime, some of the atomic rearrangements do not recover fully when the load is removed, leading to structural change, even though, at the macroscopic level, the sample returns to its original dimensions [6]. Loading MGs below the elastic limit for several hours at room temperature (RT) does induce property changes [7], but these changes can be linked to creep. In the present work, we focus instead on the instantaneous effects of elastic cycling, as first demonstrated by Packard et al. [8]. In an instrumented-indentation study, they showed that cyclic loading in the elastic range led to a 20–40% increase in the load necessary to initiate plastic flow of the MG. This substantial strengthening was attributed to 'shaking down to an 'ideal glass' configuration of higher structural order' [9]. Such an effect would be analogous to the structural relaxation induced by thermal annealing, and would indeed be of great interest as it circumvents potential problems associated with annealing, such as oxidation or crystallisation.

The present work, as for that of Packard et al. [8,9], is based on nanoindentation at a constant loading rate. By using a spherical indenter tip, the stresses and strains increase gradually upon loading, facilitating characterisation of the elastic properties and of the onset of yielding. This onset is readily detected from the first discrete displacement burst (*pop-in*) indicating the initiation and propagation of shear bands [10]. The load at the first pop-in is defined as the initial yield load F_y, and its values show a broad distribution. As reviewed in ref. [11], the distribution can be attributed to actual variation from place to place in the MG, reflecting the influence of local structural heterogeneities within the sampled volume. The yielding behaviour is represented by a cumulative distribution of F_y compiled from up to 100 loading curves and characterised by a median value and a relative width.

Packard et al. applied of order ten loading-unloading cycles in the fully elastic range (below the lowest value of F_y) to several MG compositions; subsequent indentation to detect yielding showed that the prior cycling led to an increase in the median F_y [8,9]. This strengthening saturated after ~10 cycles, occurred only when the maximum cycling load exceeded a threshold value, and was greater for cycling at higher loading rate. Atomistic MD simulations [12] and finite-element method mesoscale modelling [13] have both given cumulative distributions of F_y that show strengthening as a result of elastic cycling. The strengthening was associated with an increase in elastic modulus [12] and a reduction in free volume [13], as expected for structural relaxation of a MG.

There is interest in whether similar effects could be obtained by elastic cycling of MGs in conventional uniaxial compression of macroscopic samples (e.g. rods a few mm in diam.). Calorimetric measurements of the heat of relaxation show both decreases (indicating relaxation/*ageing*) and increases (indicating the opposite effect of *rejuvenation*). Compressive cycling over the range 37 ± 15% of the macroscopic yield stress (σ_y) induced relaxation [14], while cycling of a similar MG over the range 50 ± 37.5% of σ_y induced rejuvenation [15]. In the latter case, the microhardness (measured on the end-faces to which the compressive load

was applied) increased by up to 8%, but this effect disappeared after 45 days at RT without loading. In both these studies, the effects were attributed to anelastic strains. In any case, rejuvenation should be accompanied by a reduction not an increase in hardness.

It was suggested [15] that the strengthening resulting from elastic cycling in nanoindentation studies [8,9] might be re-interpreted as an effect of anelastic strain and residual stresses. Indeed, a nanoindentation study found that an interval of 24 s between the elastic cycling and the indentation to determine F_y, reduced the strengthening effect (the increase in the median value of F_y) by about one third [16], an effect consistent with a decay of anelastic strain.

Thermal strains in MGs should also involve non-affine displacements [17], and changes in structure and properties have been observed to result from cryogenic thermal cycling (CTC) [18]. These changes are mostly associated with rejuvenation. We have explored the opposing effects of CTC and annealing [19], and results from this companion study augment the present discussion. The same $Cu_{46}Zr_{46}Al_7Gd_1$ bulk MG is chosen for the present study. We measure the effects of elastic cycling on various states of this glass: as-cast, after CTC, and after annealing. In this way, we examine in particular the extent to which the strengthening resulting from elastic cycling in nanoindentation can be regarded as analogous to an annealing effect.

2. Experimental methods

The $Cu_{46}Zr_{46}Al_7Gd_1$ (at.%) bulk MG was prepared at the Institute of Physics, Chinese Academy of Sciences (Beijing, PR China). Master alloys were prepared by arc-melting 3–4N pure elements. A 2 mm-thick plate was obtained by induction melting and suction casting, under a Ti-gettered argon atmosphere, into water-cooled Cu-moulds. A sample with approximate dimensions of $2.5 \times 2 \times 0.5$ mm^3 was cut from this plate.

Elastic cycling was performed on three different structural states of the same sample: as-cast, after CTC and after annealing. CTC was performed as in earlier work [18,19]: the sample was dipped in liquid nitrogen for 1 min, then heated back to room temperature (RT) using an air-blower and kept at RT for 1 min. This was repeated until 10 cycles were achieved. Annealing (as in [19]) was at 633 K ($\approx 0.9\ T_g$) for 24 h, after enclosing the sample in a fused-silica tube containing titanium beads to getter oxygen, and sealed under vacuum ($\sim 10^{-3}$ mbar).

Instrumented indentation was carried out at RT on an MTS Nanoindenter XP with a diamond spherical indenter (tip radius $R = 8$ μm) under controlled loading and unloading rate of 0.5 mN s^{-1}. The maximum thermal drift rate was 0.07 nm s^{-1}. At least 40 indents were performed per sample condition, with an indent spacing of at least 20 μm to avoid overlap of strain fields. Before indentation, the as-cast sample was polished with 1-μm and ¼-μm diamond paste to a mirror finish, and then polished with a 0.06-μm colloidal silica suspension.

The sample surface was repolished with silica suspension after thermal cycling, and with diamond paste, followed by silica suspension, after annealing.

Two types of indentation loading protocols were performed: simple indentation (Figure 1(a)), consisting of monotonic loading to a maximum load F_{max} during which yielding occurred; and cyclic indentation (Figure 1(b)), consisting of six loading-unloading cycles (with a maximum cycle load F_{cyc}) in the macroscopically elastic regime, followed by loading up to F_{max}. F_{max} was chosen to be greater than F_y, and was set to 70 mN for the sample in the as-cast state and after CTC, and to 120 mN for the annealed state. F_{cyc} was set to ~50% of the median F_y determined from the simple indentation measurements: $F_{cyc} = 20$ mN for the as-cast and annealed states, and $F_{cyc} = 15$ mN for the state after CTC. With these values of F_{cyc}, there are no pop-ins during the elastic cycling, and therefore no depletion of early pop-ins in the subsequently measured distributions. From earlier work on a range of MG compositions, it is clear that, even if saturation is not reached, the greater part of the strengthening effect (increase in F_y) is already seen after five elastic cycles [8,9,16]. To constrain total measurement time and avoid instrument instabilities, we limited the present work to six loading-unloading cycles.

F_y is the load at the first pop-in event, linked to the first peak in indenter tip velocity, which corresponds to the deviation of the load-displacement curve from the Hertzian equation for elastic displacement [20]: $F = (4/3)E_r \cdot R^{1/2} \cdot h^{3/2}$, where F is the force, h the tip displacement and E_r the indentation modulus. The initial yield pressure P_y is defined as $P_y = F_y/(\pi R h_y)$, where h_y is the displacement at the initial pop-in. E_r is determined by inserting F_y and h_y into the Hertzian equation and solving for E_r. The hardness is calculated from $H = F_{max}/(\pi a^2)$, with the radius of the circle of contact $a = \sqrt{2Rh_c - h_c^2}$ and $h_c = (h_{max} + h_f)/2$ [21], where h_{max} is the displacement at F_{max} and h_f is the depth of the residual impression. A further property measured here is Δh, defined as the increase in displacement at constant load during the first pop-in.

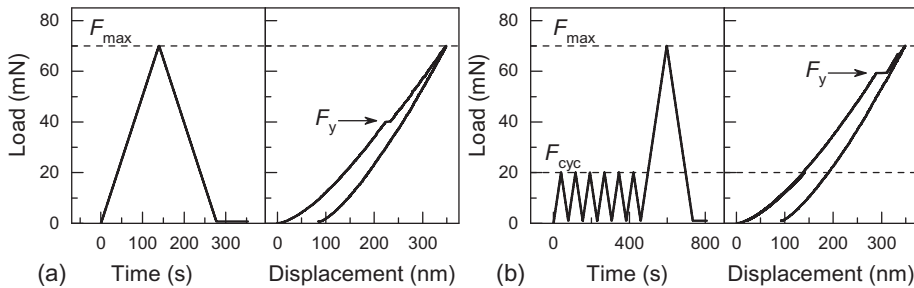**Figure 1.** For the as-cast sample of $Cu_{46}Zr_{46}Al_7Gd_1$ bulk metallic glass, example nanoindentation loading protocols and resulting load-displacement curves for: (a) a simple indentation; and (b) cyclic elastic loading followed by indentation.

After the initial yield event at F_y on each loading curve, further pop-ins occurred upon loading up to F_{max}. An average velocity v was calculated (as in Ref. [22]) to describe the behaviour of all pop-ins occurring during each loading. To calculate v, a constant C, corresponding to the mean velocity if no pop-ins had occurred, was subtracted from the indenter velocity $v_{ind} = dh/dt$, where t is the time, then $(v_{ind} - C)$ was integrated as a function of h from 50 nm to h_{max}; this was finally divided by $(h_{max} - 50$ nm$)$. The first 50 nm of the indentation was disregarded for calculating v, as v_{ind} is high at the start of the indentation until a good contact is made between the indenter tip and sample surface.

3. Results

3.1 Properties related to the initiation of flow

In the companion study [19] of the effects of CTC and annealing on the $Cu_{46}Zr_{46}Al_7Gd_1$ MG, the results were rationalised by considering the MG in terms of dispersion of soft spots in a relatively rigid matrix. Some properties $(F_y, P_y, \Delta h, v)$ are related to the initiation of flow, and are sensitive to the soft
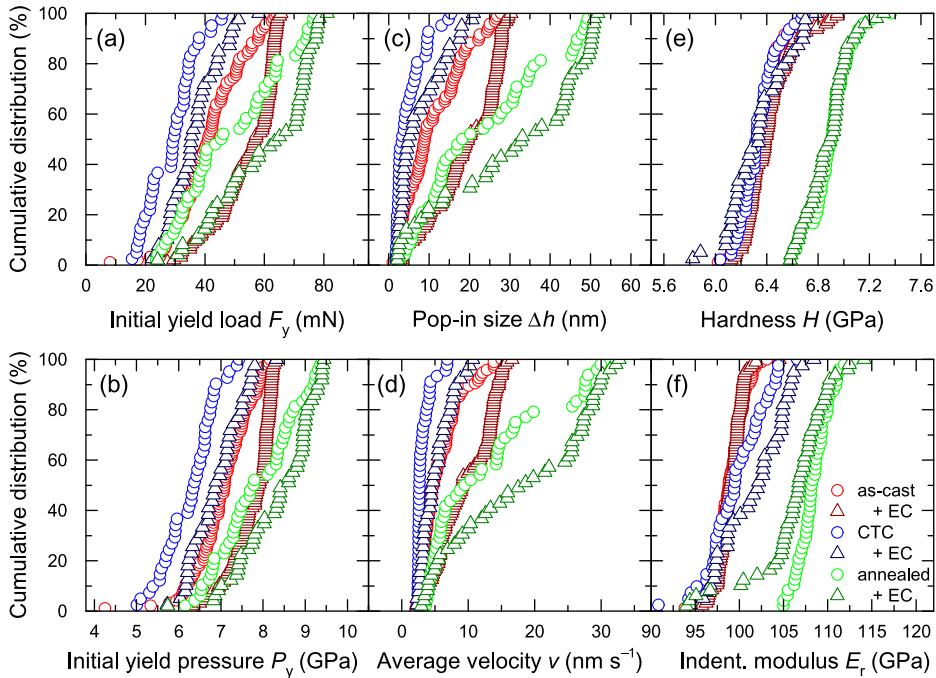
Figure 2. (Colour online) From multiple loading curves for nanoindentation of $Cu_{46}Zr_{46}Al_7Gd_1$ bulk metallic glass in its as-cast state, and after various combinations of elastic cycling (EC), cryogenic thermal cycling (CTC) and annealing, cumulative distributions of: (a) initial yield load F_y; (b) initial yield pressure P_y; (c) initial pop-in size Δh; (d) average indenter velocity v during pop-ins; (e) hardness H; and (f) indentation modulus E_r.

spots as influenced mainly by CTC, while other properties (H, E_r) are sensitive to the matrix as influenced mainly by annealing. Figure 2 shows cumulative distributions for each of the properties measured from the nanoindentation loading curves; the median values (i.e. at the 50% percentile) of these distributions, and their relative widths, are given in Table 1. The relative widths are defined to be ± half of the range from the 1st to 9th decile, divided by median value.

For the first set of properties (F_y, P_y, Δh, v), the average relative widths of the cumulative distributions (Figure 2) are ±12% for P_y, ±35% for F_y, and even greater for Δh and v. For the second set of properties (H, E_r) the average relative width is ±3%. It is expected that the relative width would be much greater for those properties dependent on local heterogeneities, mainly because of the stochastic variation of the population of these heterogeneities in the relevant volume under the indenter tip. The difference in relative width between the two sets of properties is relevant when considering the shifts of median values; for example a 10% increase in F_y would be regarded as small (relative to the width of the distribution), whereas a 10% increase in H would be large. When including the effects of elastic cycling (EC) in this study, the division into two types of property remains clear, and EC appears to belong with CTC in affecting mainly the initiation of flow.

The as-cast MG has a median F_y of 41.2 mN; this is reduced by 28%, to 29.7 mN, by CTC, and increased by 11%, to 45.8 mN, by annealing (Figure 2(a)). These results, reported earlier [19], can be compared with the effect of elastic cycling (EC), which increases the median F_y by 39%, to 57.2 mN, consistent with the strong effect found by Packard et al. [8,9,16]. EC when applied to the MG after CTC induces a 19% increase in median F_y, and when applied to the annealed MG induces a 42% increase (Figure 2(a), Table 1).

Table 1. Obtained from multiple loading curves in nanoindentation, the cumulative distributions for initial yield load F_y, initial yield pressure P_y, initial pop-in size Δh, average velocity during pop-ins v, hardness H, and indentation modulus E_r, are characterised by the median property value and the relative width of the distribution, defined to be ± half of the range from the 1st to 9th decile, divided by median value.

Property	As-cast	+ EC	CTC	+ EC	Annealed	+ EC
F_y (mN) ± 0.1 median	41.2	57.2	29.7	36.5	45.8	65.0
relative width (%)	±38	±23	±33	±31	±51	±31
P_y (GPa) ±0.04 median	7.08	7.91	6.38	6.89	7.79	8.61
relative width (%)	±12	±8	±10	±11	±17	±14
Δh (nm) ± 0.2 median	9	20	3	5	19	33
relative width (%)	±110	±55	±111	±160	±109	±71
v (nm s^{-1}) ± 1 median	5	9	3	5	10	19
relative width (%)	±85	±59	±36	±65	±119	±70
H (GPa) ± 0.003 median	6.360	6.385	6.325	6.346	6.908	6.903
relative width (%)	±2.8	±3.4	±3.1	±4.8	±3.3	±3.2
E_r (GPa) ±0.04 median	98.82	99.03	99.52	102.20	108.2	106.74
relative width (%)	±2.1	±1.5	±3.9	±4.5	±2.2	±4.7

Note: These characteristics are given for $Cu_{46}Zr_{46}Al_7Gd_1$ bulk metallic glass in its as-cast state, and after cryogenic thermal cycling (CTC) and annealing. In addition, the effect of elastic cycling (EC) on each of these states is shown.

Similar trends on applying CTC, annealing and EC are seen for P_y (Figure 2 (b)), and these are broadly similar also for Δh and v (Figure 2(c,d)), although the shape of the cumulative distributions is different in those cases. EC clearly increases the median values of F_y, P_y, Δh and v, but for as-cast and annealed samples, the lowest and highest values in the cumulative distribution are hardly increased. When applied to the MG after CTC treatment, however, EC shifts the entire distributions of F_y and P_y to higher values, and shifts the distributions for Δh and v progressively more for higher values of Δh and v.

3.2 Properties related to the metallic-glass matrix

While F_y and P_y characterise the conditions for the initiation of plastic flow, H is relevant for ongoing flow, and is, therefore, less sensitive to the inhomogeneity of the MG [19]. The as-cast MG has a median H of 6.360 GPa; this is essentially unchanged by CTC, increased 9% by annealing, and unchanged by EC (Figure 2(e)). EC of the MG has no effect on the median H when applied after CTC or after annealing.

EC has similarly little effect on the median value of E_r, but it does slightly increase the upper values when applied to the CTC-treated sample and decrease the lower values when applied to the annealed sample. Annealing increases the median E_r, by ~9% (Figure 2(f), Table 1). The distributions of H and E_r show the effects of EC and of annealing to be very different. The distinction between EC and annealing is also evident in comparing their effects, on the as-cast glass, in the two suggested regimes influenced mainly by the soft spots or by the rigid matrix. EC increases median F_y but has no effect on H; in contrast, annealing has relatively little effect on median F_y but increases H.

In the companion paper [19], it is reported that the ratio H/E_r is very similar, $(6.38 \pm 0.02) \times 10^{-2}$, in all states (as-cast, CTC-treated, and annealed) of the $Cu_{46}Zr_{46}Al_7Gd_1$ MG, and for other MGs also. This ratio is proportional to the yield strain, which is often considered constant for MGs [23]. In the present work, after applying EC to as-cast, CTC-treated, and annealed states, $H/E_r = (6.37 \pm 0.06) \times 10^{-2}$. We conclude that this ratio is effectively universal for MGs, describing the conditions for ongoing macroscopic plastic flow.

In contrast, the ratio F_y/E_r (measured with typical SD error of ±0.001) is not constant, varying from 0.417 for the as-cast MG, to 0.298 after CTC, 0.423 after annealing, and 0.266 after annealing and CTC [19]. In the present work, the ratio is 0.577 after EC, and 0.609 after annealing and EC. There is thus a clear pattern that CTC reduces the barrier to initiation of flow (by ~30%), while EC increases it (by ~40%).

3.3 Induced changes in the difficulty of initiating plastic flow

The initial yield pressure P_y is proportional to the indentation modulus E_r and to the radius a of the circle of contact of the spherical tip. Underneath the tip, the

indentation zone in which the induced strains and stresses are significant has linear dimensions that scale with a [24]. We may expect that the pop-in size Δh would also depend on E_r and a. Indeed, P_y and Δh are correlated (Figure 3), the datasets for the different states of the MG superposing to give a universal curve (Figure 3(a)). Such a superposition is not found for other plots (F_y–h_y, F_y–Δh, P_y–h_y, or h_y–Δh, not shown). Although there is, broadly, a universal P_y–Δh curve, the datasets for different MG states populate different parts of the curve. CTC of the as-cast MG shifts the dataset to lower values of P_y on the curve. In contrast, annealing removes the lowest values of P_y, and shifts the dataset so that the P_y–Δh curve is significantly extended to higher values of P_y. EC of the as-cast MG removes the lowest values of P_y, and gives more points with high values of P_y, but otherwise, the curve is not affected (Figure 3(b)). EC of the CTC-treated MG shifts the dataset back up to higher values of P_y on the curve (Figure 3(c)). EC of the annealed MG shifts the data to somewhat higher P_y values on the curve (Figure 3(d)).

The P_y–Δh plots (Figure 3) show small populations of pop-ins that occur at small Δh (2–4 nm) with P_y values far from the main curve. Those with P_y values below the main curve are most evident for the as-cast glass and after CTC. These occur before expected yielding and presumably result from stress
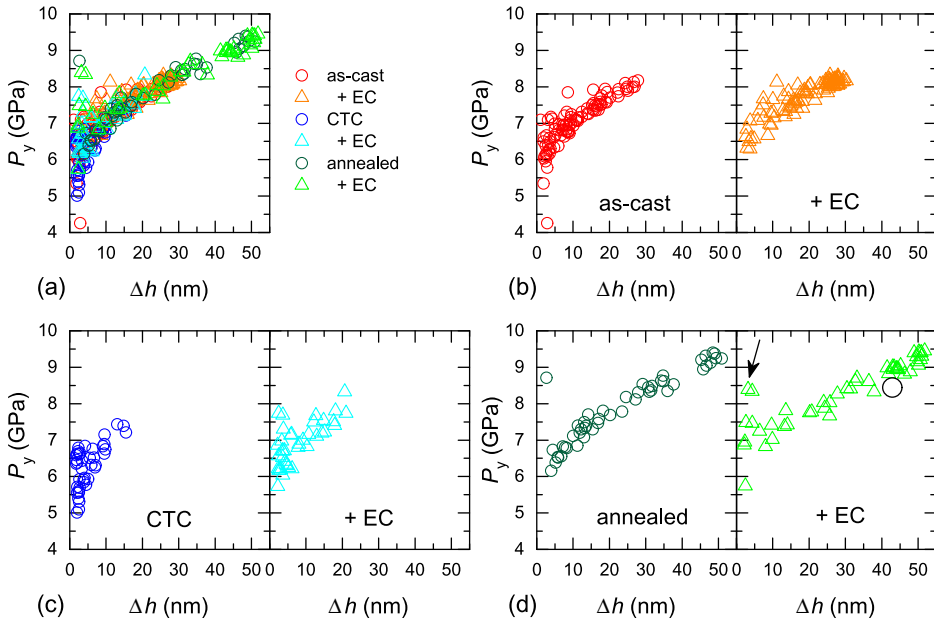

Figure 3. (Colour online) Relationship between the initial yield stress P_y and the displacement increment Δh during the initial pop-in: (a) for all sample states; and for the effects of elastic cycling (EC) on (b) the as-cast MG; (c) the MG subjected to cryogenic thermal cycling (CTC); and (d) the annealed MG. In (d), the arrow highlights an example of an initial pop-in that is much smaller than would be expected for its P_y value; the P_y and Δh values of the subsequent pop-in on the same loading curve are indicated by the open circle.

concentration at local heterogeneities. Of more interest is the population of low-Δh pop-ins with P_y values above the main curve. On P_y–h_y plots the corresponding outliers do not exist; the behaviour is as expected for the Hertzian solution in the elastic regime. The outlier points in P_y–Δh plots thus represent yielding at expected values of h_y, but with abnormally small pop-ins, as considered further in §4.1.

4. Discussion

4.1 Volume affected by elastic cycling

Pop-ins reflect the initiation and propagation of shear bands. Packard et al. [8] note that propagation must ultimately involve following a path to the sample surface with the yield stress exceeded along the entire path. In the present case, the yielding under indentation is clearly affected by the treatments applied to the samples (EC, annealing, CTC) even though the sample surface is freshly prepared in each case. Thus, the internal state of the MG is more important than its surface in governing the initiation of yield.

In particular, any effects of EC must relate to the strains under the indenter tip. As noted above, the dimensions of the indentation zone scale with the contact radius a. Assuming that the strains are predominantly elastic, a is proportional to $F^{1/3}$, and therefore the volume of the indentation zone is proportional to F. The maximum load in EC, F_{cyc}, was 15 or 20 mN, while the maximum load, F_{max}, at end of the subsequent loading curve was 70 or 120 mN. The conditions at F_{max} are relevant for the determination of H. At that point, F_{max}/F_{cyc} is in the range 3.5–6.0. Thus, only 17–29% of the zone volume at F_{max} could have been affected by the prior EC, and this would be relevant only in the early stages of the indentation. Whatever the possible effect of the EC on the MG structure, EC is expected to have no effect on the measured value of H (as is confirmed in Figure 2(e)).

The indentation modulus E_r is determined by fitting the loading curve up to F_y (the initial pop-in). F_{cyc} was selected so that at the median of the distribution $F_y/F_{cyc} \approx 2$. If EC did relax the MG in the indentation zone, this would cause the modulus in that zone to increase, and that should be detectable as an increased E_r (as is seen on annealing, Figure 2(f)). For the as-cast MG, EC has essentially no effect on E_r. For the annealed MG, EC causes a small decrease in median E_r that is in marked contrast with the strong increase that it causes in median F_y. While overall the effects of EC on E_r (Figure 2(f)) are difficult to interpret, they are certainly not consistent with increasing the modulus in the indentation zone.

On loading, the greatest stresses are at ~0.5 a below the indenter tip [24]. If EC strengthens the MG in any way, the strengthening would be local, and the initial yielding on subsequent loading would occur in a non-uniform region. After EC, there is an increased population of pop-ins that are much smaller

than would be expected from the associated values of P_y and h_y. These abnormally small pop-ins may be cases in which propagation of shear is blocked by local strengthening induced by the prior EC. Each small pop-in is followed by a pop-in that does lie on the universal P_y–Δh curve; one example is indicated in Figure 3(d). Otherwise, there are no examples of pop-ins being followed by much larger ones. The possible origins of local strengthening are considered next (§4.2 and §4.3).

4.2 F_y as a measure of the degree of relaxation of the glass

When it was suggested that elastic cycling could induce relaxation of the MG to states of higher order, it was pointed out that the states might be different from those attainable by annealing [9]; nevertheless, relaxation, however induced, should lead to qualitatively similar changes, for example increases in the density of the MG and in its resistance to plastic flow. Packard et al. [11] noted that the effect of annealing on the strength of their MGs was 'extremely subtle' (i.e. weak), but assessed the strength only in terms of F_y. The present results (Figure 2(a)) confirm that annealing has relatively little effect on median F_y. But, as shown by the significant increase in H (Figure 2(e)), it is not true that annealing has little effect on strength. Indeed, we conclude that, compared to H, F_y is relatively insensitive to the degree of relaxation of the glass, and accordingly that changes in F_y cannot be used to assess the degree of relaxation (contrary to the implication by Packard et al. [8,9,11,16]).

As seen in Figure 2(a), EC applied to all states of the MG induces an increase in F_y, an effect expected to be associated with relaxation of the MG structure. But, in the context of relaxation, it is inexplicable that the smallest effect is when EC applied to a rejuvenated (CTC-treated) glass and the largest effect is when applied to a relaxed (annealed) glass, especially since the MG was expected to be fully relaxed after the annealing in the present work. And, as noted above, a large further relaxation of the annealed MG would give an increase in E_r, which is not observed. The atomistic simulation reproducing the strengthening [12] did not reveal any obvious signs of structural change, but may have shown relaxation (indicated by the increase in elastic modulus) under elastic cycling because the simulated as-cast glass is so unrelaxed.

4.3 Possible anelastic effects on F_y

When indenting the surface of an MG, the measured microhardness is higher if the surface is in biaxial compression [25]. Such effects are expected to be greater in materials, such as MGs, that have relatively high values of yield strain [26]. In previous work, the surface residual stress arose from plastic deformation as the surface was shot-peened [25], and the depth of the microhardness indents was much less than the depth of the deformed surface layer.

We now consider the possible effects of EC. If the elastic strains induced during EC were instantaneously recovered, then the EC could not induce any residual stress. But metallic glasses show distinct anelasticity [6], and it is expected that not all of the strain would be instantaneously recovered. Then, the result of the EC would be a zone under the indent site, of residual stress that would be compressive and would decay with time. And, in that case, we would expect that EC could lead to increases in F_y, P_y, Δh and v, when indenting is continued at that site.

As already noted, delaying the resumption of loading after EC, reduces the induced increase in F_y [16]. This suggests that in nanoindentation studies of the present type, the extent by which F_y is increased by EC might be largely dependent on the extent of the decay of anelastic strain; greater decay means less residual strain and smaller induced increase in F_y. Such a spontaneous decay would, of course, be impossible if the effect induced by EC was a relaxation of the MG into a more stable, more ordered structure.

The rate of anelastic decay would depend on the degree of relaxation of the MG. If relaxed by annealing, the decay is slower, and if treated by CTC the decay is faster [27]. On this basis, we have a qualitative explanation for the EC effects on median F_y. The increase in F_y is least for the CTC-treated sample because the anelastic strain has decayed the most and, in contrast, the increase is greatest for the annealed sample, in which the strain has decayed the least. That the increase in F_y is greater upon EC at a higher loading rate [8,9] is readily explained, as at higher rate there is less time for anelastic decay. The effects discussed above for F_y (Figure 2(a)) are also found for P_y, Δh and v (Figure 2(c,d)).

In accordance with the analysis of Packard et al. [11], we take the widths of the cumulative distributions to be due to heterogeneity of the MG samples. It is consistent for F_y, P_y, Δh and v (Figure 2(a–d)), that, when applied to the as-cast and annealed states, EC causes the biggest increase around the median value, and has only a slight effect on the weaker regions (i.e. the lower end of the distributions), and no effect on the stronger regions (i.e. the upper end). In the stronger regions, the initial pop-in occurs at an F_y increasingly larger than F_{cyc}, The higher the value of F_y/F_{cyc}, the less the pop-in would be affected by the relatively shallow region of residual stress induced by the EC. And for initial pop-ins at large enough F_y, prior EC should have no effect.

The small effect of EC in the weaker regions is more difficult to explain. In these regions, however, the atomic mobility is presumed to be higher, and any anelastic decay would be faster, limiting the induced strengthening.

This effect, that the biggest increases in F_y, P_y, Δh and v induced by EC are around the median property values, is not found for the MG subjected to CTC. The lower median values induced by CTC, and the generally smaller spread of values (i.e. narrower distribution), suggest that initial yield is easier and more uniform within the MG. Due to this greater uniformity of yielding in the CTC-treated MG, all indented regions are affected by EC to a similar degree.

As noted by Packard et al. [8], the strengthening effect is seen after EC, while there is little or no effect after apparently equivalent static loading in the elastic regime. Even if the strengthening is due to induced anelastic strain, there remain questions about why cycling has a much stronger effect than static loading.

5. Conclusions

Elastic cycling (EC) under a nanoindenter tip has been reported to cause local strengthening of a metallic glass (MG), and it was proposed that the strengthening is due to structural relaxation of the glass stimulated by a mechanical 'shaking down'. For $Cu_{46}Zr_{46}Al_7Gd_1$ bulk MG, we have used nanoindentation to compare the effects of EC with those of annealing and of cryogenic thermal cycling (CTC). Cumulative distributions have been measured for the initial yield load F_y, yield pressure P_y, and pop-in size Δh, for average pop-in velocity v, for hardness H, and for indentation modulus E_r. The distributions for F_y, P_y, Δh and v are wide, related to the onset of plastic flow possibly mediated by soft spots in the MG. In contrast, the distributions for H and E_r are narrow, related to the relatively stiff matrix within which the soft spots are dispersed.

We confirm that EC does have a strong effect in raising F_y, but this effect is greatest when the EC is applied to a MG relaxed by annealing, and least when applied to a MG rejuvenated by cryogenic thermal cycling. The large increase in F_y is not accompanied by an increase in E_r. These results are not consistent with the effects of EC being qualitatively similar to those of annealing. We conclude that, anyway, F_y is relatively insensitive to the state of relaxation of the MG.

We propose that the apparent strengthening as a result of EC is due to induced anelastic strains and consequent compressive residual stresses that oppose the initiation of plastic flow. The extent of strengthening may then be decreased by time-dependent decay of the anelastic strains. Such effects can qualitatively explain a greater increase in F_y for greater maximum load in EC, for greater loading rate in EC, and for shorter delay between EC and continued loading to initiate flow. They also explain why EC induces the greatest increase in F_y for the annealed MG and the least increase for the CTC-treated glass.

There may be effects of elastic cycling on the state of structural relaxation of MGs, but they are not demonstrated in studies of cycling in nanoindentation.

Disclosure statement

No potential conflict of interest was reported by the authors.

ORCID

C. M. Meylan http://orcid.org/0000-0001-9951-8085
A. L. Greer http://orcid.org/0000-0001-7360-5439

References

[1] D. Weaire, M.F. Ashby, J. Logan, and M.J. Weins, *On the use of pair potentials to calculate the properties of amorphous metals*, Acta Metall. 19 (1971), pp. 779–788.

[2] H.F. Poulsen, J.A. Wert, J. Neuefeind, V. Honkimäki, and M. Daymond, *Measuring strain distributions in amorphous materials*, Nat. Mater. 4 (2005), pp. 33–36.

[3] T.C. Hufnagel, R.T. Ott, and J. Almer, *Structural aspects of elastic deformation of a metallic glass*, Phys. Rev. B 73 (2006), Article ID: 064204.

[4] U.K. Vempati, P.K. Valavala, M.L. Falk, J. Almer, and T.C. Hufnagel, *Length-scale dependence of elastic strain from scattering measurements in metallic glasses*, Phys. Rev. B 85 (2012), Article ID: 214201.

[5] J. Ding, Y.Q. Cheng, and E. Ma, *Correlating local structure with inhomogeneous elastic deformation in a metallic glass*, Appl. Phys. Lett. 101 (2012), Article ID: 121917.

[6] T. Egami, T. Iwashita, and W. Dmowski, *Mechanical properties of metallic glasses*, Metals 3 (2013), pp. 77–113.

[7] A.L. Greer and Y.H. Sun, *Stored energy in metallic glasses due to strains within the elastic limit*, Philos. Mag. 96 (2016), pp. 1643–1663.

[8] C.E. Packard, L.M. Witmer, and C.A. Schuh, *Hardening of a metallic glass during cyclic loading in the elastic range*, Appl. Phys. Lett. 92 (2008), Article ID: 171911.

[9] C.E. Packard, E.R. Homer, N. Al-Aqeeli, and C.A. Schuh, *Cyclic hardening of metallic glasses under Hertzian contacts: Experiments and STZ dynamics simulations*, Philos. Mag. 90 (2010), pp. 1373–1390.

[10] J.H. Perepezko, S.D. Imhoff, M.W. Chen, J.Q. Wang, and S. Gonzalez, *Nucleation of shear bands in amorphous alloys*, Proc. Natl. Acad. Sci. USA 111 (2014), pp. 3938–3942.

[11] C.E. Packard, O. Franke, E.R. Homer, and C.A. Schuh, *Nanoscale strength distribution in amorphous versus crystalline metals*, J. Mater. Res. 25 (2010), pp. 2251–2263.

[12] C. Deng and C.A. Schuh, *Atomistic mechanisms of cyclic hardening in metallic glass*, Appl. Phys. Lett. 100 (2012), Article ID: 251909.

[13] N. Wang, F. Yan, and L. Li, *Mesoscopic examination of cyclic hardening in metallic glass*, J. Non-Cryst. Solids 428 (2015), pp. 146–150.

[14] A. Caron, A. Kawashima, H.-J. Fecht, D.V. Louzguine-Luzgin, and A. Inoue, *On the anelasticity and strain induced structural changes in a Zr-based bulk metallic glass*, Appl. Phys. Lett. 99 (2011), Article ID: 171907.

[15] D.V. Louzguine-Luzgin, V.Y. Zadorozhnyy, S.V. Ketov, Z. Wang, A.A. Tsarkov, and A.L. Greer, *On room-temperature quasi-elastic mechanical behaviour of bulk metallic glasses*, Acta Mater. 129 (2017), pp. 343–351.

[16] N. Al-Aqeeli, *Strengthening behavior due to cyclic elastic loading in Pd-based metallic glass*, J. Alloys Comp. 509 (2011), pp. 7216–7220.

[17] T.C. Hufnagel, *Cryogenic rejuvenation*, Nat. Mater. 14 (2015), pp. 867–868.

[18] S.V. Ketov, Y.H. Sun, S. Nachum, Z. Lu, A. Checchi, A.R. Beraldin, H.Y. Bai, W.H. Wang, D.V. Louzguine-Luzgin, M.A. Carpenter, and A.L. Greer, *Rejuvenation of metallic glasses by non-affine thermal strain*, Nature 524 (2015), pp. 200–203.

[19] C.M. Meylan, F. Papparotto, S. Nachum, J. Orava, M. Miglierini, V. Basykh, J. Ferenc, T. Kulik, and A.L. Greer. *Stimulation of shear-transformation zones in metallic glasses by cryogenic thermal cycling*, J. Non-Cryst. Solids 548 (2020), Article ID: 120299.

[20] K.L. Johnson, *Contact Mechanics*, Cambridge University Press, Cambridge, 1985.

[21] J.S. Field and M.V. Swain, *A simple predictive model for spherical indentation*, J. Mater. Res. 8 (1993), pp. 297–306.

[22] P. Denis, C.M. Meylan, C. Ebner, A.L. Greer, M. Zehetbauer, and H.J. Fecht, *Rejuvenation decreases shear band sliding velocity in Pt-based metallic glasses*, Mater. Sci. Eng. A 684 (2017), pp. 517–523.

[23] W.L. Johnson and K. Samwer, *A universal criterion for plastic yielding of metallic glasses with a $(T/T_g)^{2/3}$ temperature dependence*, Phys. Rev. Lett. 95 (2005), Article ID: 195501.

[24] S. Pathak and S.R. Kalidindi, *Spherical nanoindentation stress-strain curves*, Mater. Sci. Eng. R 91 (2015), pp. 1–36.

[25] Y. Zhang, W.H. Wang, and A.L. Greer, *Making metallic glasses plastic by control of residual stress*, Nat. Mater. 5 (2006), pp. 857–860.

[26] X. Chen, J. Yan, and A.M. Karlsson, *On the determination of residual stress and mechanical properties by indentation*, Mater. Sci. Eng. A 416 (2006), pp. 139–149.

[27] C.M. Meylan, *Thermomechanical processing of metallic glasses*, Ph.D. thesis, University of Cambridge, 2019.